Improvement of methods for studying internal gravity waves in the Earth's atmosphere using radiosonde measurements

Improvement of methods for studying internal gravity waves in the Earth's atmosphere using radiosonde measurements

V N Gubenko[1], **I A Kirillovich**[1] **and V E Andreev**[1]

[1] Kotel'nikov Institute of Radio Engineering and Electronics RAS (Fryazino branch), Vvedensky square 1, Fryazino 141190, Moscow region, Russia

E-mail: vngubenko@gmail.com, gubenko@fireras.su

Abstract. Internal gravity waves (IGWs) determine atmospheric dynamics at all heights providing an effective mechanism for the transfer of wave energy and momentum upward from the lower levels. The dynamical (shear) and convective instabilities contribute most to the energy dissipation and saturation of internal waves in the Earth's atmosphere. The wave saturation assumption is a key point at the radio occultation (RO) investigations of IGWs, therefore, verification of its implementation in the Earth's atmosphere using radiosonde studies is an important task of atmospheric physics. We propose an upgraded hodograph method based on combined analysis of the velocity and temperature measurements. To achieve the minimal errors in obtained results of reconstructing the internal wave characteristics, the polarization relation between the wave wind speed and temperature variations in the Earth's atmosphere has been used. It has been shown that the improved method of wind speed hodograph analysis is especially relevant for cases when the intrinsic frequencies of analyzed IGWs noticeably exceed the Coriolis parameter values.

1. Introduction

Classical hodograph method has been widely used to analyze the quasi-monochromatic IGWs observed by radars, lidars, radiosondes, ground-based observations of airglow, and by satellite instruments [1–23]. The main purpose of the atmospheric dynamics is to investigate internal gravity waves which determine the atmospheric dynamics at all heights [24–27]. It is known that the traveling ionospheric disturbances (TIDs) and sporadic E-layers in the Earth's ionosphere are wave manifestations in the neutral atmosphere. The RO measurements at terrestrial atmospheres are a powerful instrument of wave activity research. These RO studies of internal waves analyze measurements from one surveillance system. It gives a possibility to analyze only one independent value. While the literature is very rich on the experimental IGW studies, only few studies so far considered both the wind and temperature fluctuations at the same time. So, authors of the work [10], using the Na-lidar measurements in the mesopause region, analyzed propagating internal waves in individual profiles of simultaneous wind and temperature variations and found the same downward phase speed in both sets of profiles.

Simultaneous velocity and temperature data found from the balloon measurements allow to know more about the role of IGWs at the atmospheric dynamics. The sonde measurements give a possibility to check the RO investigations of internal waves which are based at an analysis of wave-like temperature or density variations using a saturated wave assumption (SWA-technique). By measuring and analyzing the temperature and velocity perturbations, one can find a wave saturation degree, and

thus, estimate the potency of SWA-technique [28]. In these wave investigations, we put into practice an advanced hodograph technique that relies on the velocity and temperature analysis and uses the polarization equation between temperature and velocity perturbations for IGWs. This improved method of wind speed hodograph analysis is especially relevant for cases when the intrinsic frequencies noticeably exceed the values of Coriolis parameter (inertial frequency), and it gives a possibility to achieve the minimal uncertainties at results of reconstructing the IGW parameters.

2. Basic equations for internal waves and improved method of wind speed hodograph analysis

A detailed description of the theoretical background for internal atmospheric waves has been given in the works [24–34]. The basic wave equations have been derived in [28] and their further development is presented in this paper. The idea of the classical hodograph analysis method (HA-method) involves monitoring the motion of the velocity perturbations vector versus altitude [33]. Drawing of elliptical wind hodographs versus time or altitude are widely used for the IGW studies [14]. It is important to note that the practical application of classical hodograph method for an analysis of radiosonde wind speed measurements in the Earth's atmosphere encounters difficulties in cases when the intrinsic frequencies (ω) of analyzed IGWs noticeably exceed the Coriolis parameter (f) values (for example, $\omega>5f$). Here, according to polarization relation (2) from the work [28], the f/ω ratio will be small (<0.2), and the standard accuracy (~1 m/s) of determining the wind speed in radiosonde measurements may not be sufficient for qualitative restoration of the frequency ω from indicated relation (2). We will illustrate the above with the following example: let the measured length of major semi-axis of the polarization ellipse be ~5 m/s. Then, for the case f/ω =0.2, we find that the length of minor semi-axis of the ellipse is equal to ~1 m/s. However, the relative error in finding this value is of ~100%, and it also determines accuracy of calculating the f/ω ratio and intrinsic frequency ω from the polarization relation (2) in [28]. In addition, the use of more accurate expression (6) from the work [28] for reconstructing wave characteristics imposes an additional restriction f/ω <0.1 on the range of ω-values, regardless of how accurately the wind speed is determined in radiosonde measurements.

We offer an improved version of the classical hodograph method, which is based on the combined data analysis (CDA-method) of the temperature and velocity measurements. The accuracy of temperature determination in sonde measurements is rather high and equal to ~0.2 K. To achieve minimal errors in the results of reconstructing the characteristics of internal waves, polarization equation between the atmospheric IGW perturbations of wind velocity and temperature is used [28]. Here, the ratio f/ω and intrinsic frequency ω are calculated with a good accuracy using the experimentally determined amplitudes of the normalized temperature $\left|\hat{T}'\right|$ and wind speed $|u'|$ variations. The upgraded method for analyzing the wind speed hodograph is relevant for cases when the intrinsic frequencies of IGWs substantially exceed the Coriolis parameter values.

3. Analysis of experimental data by the improved hodograph method

To show the potency of the improved hodograph technique, let us consider its application to an analysis of the radiosonde temperature and velocity measurements at Earth's stratosphere. Analyzed data were recorded each 6 s, and they are freely available on the website of the SPARC (Stratospheric Processes And their Role in Climate) Data Center.

Figure 1 demonstrates examples of the nearly co-located radiosonde wind speed and temperature data and FORMOSAT-3/COSMIC RO temperature data obtained on 30 November 2007 in the atmosphere over Kodiak, Alaska. These radiosonde and RO soundings with spatial separations < 120 km and within 12 hours demonstrate, in general, an agreement in the altitude interval from 9 to 26 km. Vertical correlation of wave-like variations of temperature with altitude (interval indicated by dashed lines) is visible from two radiosonde soundings performed with the temporal separation of ~12 hrs. Indicated correlation at the abovementioned altitude range assumes that analyzed perturbations can be caused by the semidiurnal tide or the internal wave having a ground-based period of ~12 hrs / n , where n is

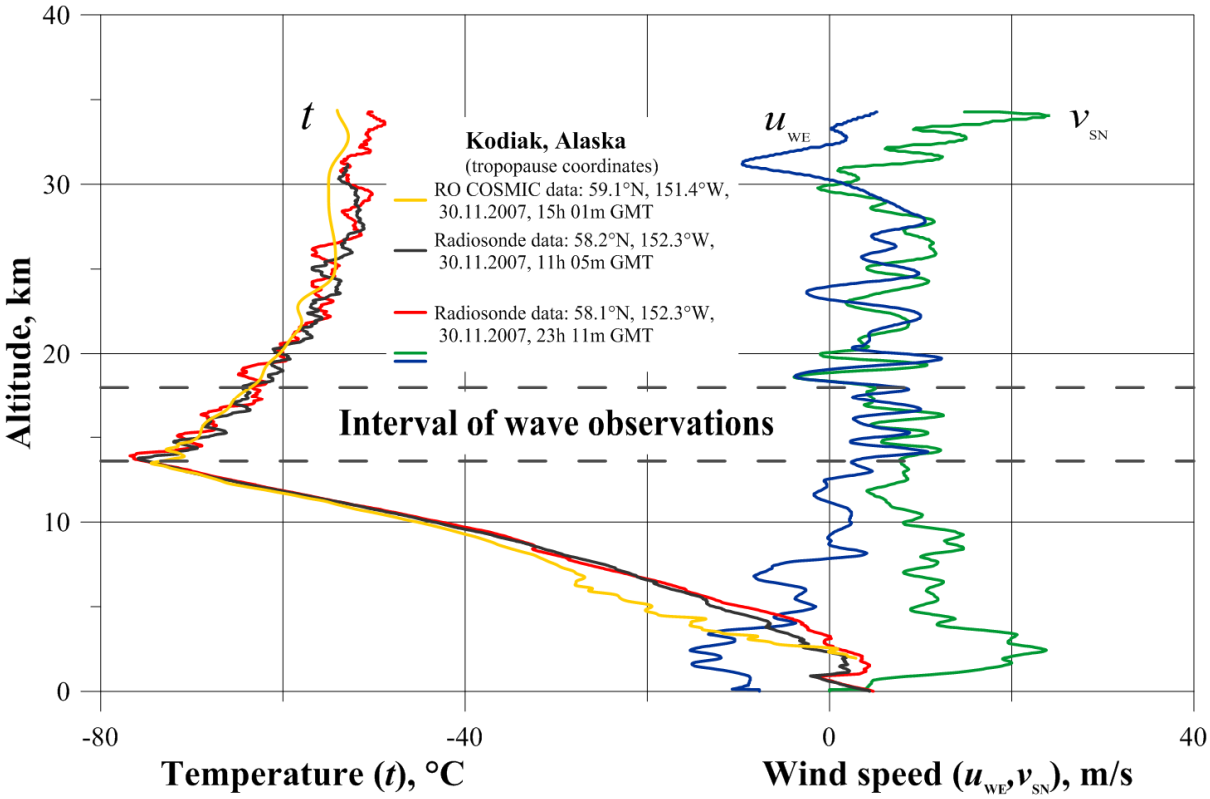

Figure 1. Examples of nearly co-located radiosonde wind speed and temperature data and RO COSMIC temperature data obtained on 30 November 2007 in the atmosphere over Kodiak, Alaska. These radiosonde and RO soundings with spatial separations < 120 km and within ~12 hrs demonstrate, in general, an agreement in the altitude interval from 9 to 26 km. Vertical correlation of wave-like temperature variations with altitude (interval indicated by dashed lines) is visible from two radiosonde soundings performed with the temporal separation of ~12 hrs.

a natural number. To check indicated assumption, let us provide a combined data analysis of the temperature (left panel in Figure 1) and the wind velocity (right panel in Figure 1) measurements for the 30 November 2008 (23h 11m GMT).

Figure 2 shows the dependencies for the selected altitude range 13.5–18 km of the wave-like perturbations. The background or mean dependencies, found by using the LSM-approximation of the raw data with the aid of 3rd-degree polynomial, are indicated by dotted lines. An application of equation (5) from the work [28] to the background temperature dependence gives a possibility to determine the mean buoyancy frequency N_b=2.58·10^{-2} rad/s for the analyzed altitude range.

The first step of data analysis is to remove the background from the original data. The background removal procedure plays a key role in the IGW analysis techniques and may even lead to strongly biased results. Figure 3 shows dependencies of the wind velocity and temperature variations versus altitude, which are determined as differences between the raw and background profiles. From determined dependencies, we find the temperature perturbations amplitude $|T'|$=2.3 K and the vertical wavelength λ_z=1.1 km for temperature and wind velocity perturbations. We choose the altitude range to plot the wind velocity hodograph and estimate the mean temperature T_b=203 K at the center of the specified range on altitude of ~14.7 km.

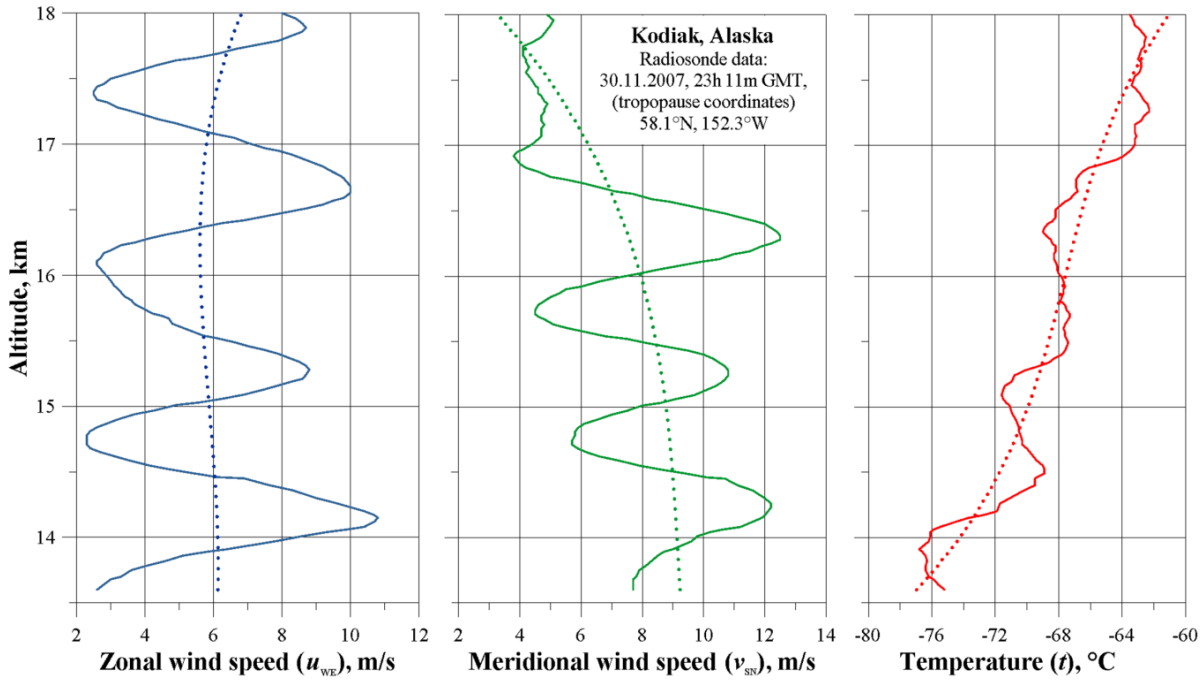

Figure 2. Vertical profiles of temperature, zonal and meridional wind speed components obtained from simultaneous radiosonde measurements on 30 November 2007 in the atmosphere over Kodiak, Alaska. Background (mean) profiles determined from the raw data by a least-square cubic polynomial fit within the interval of wave observations are shown by dotted lines.

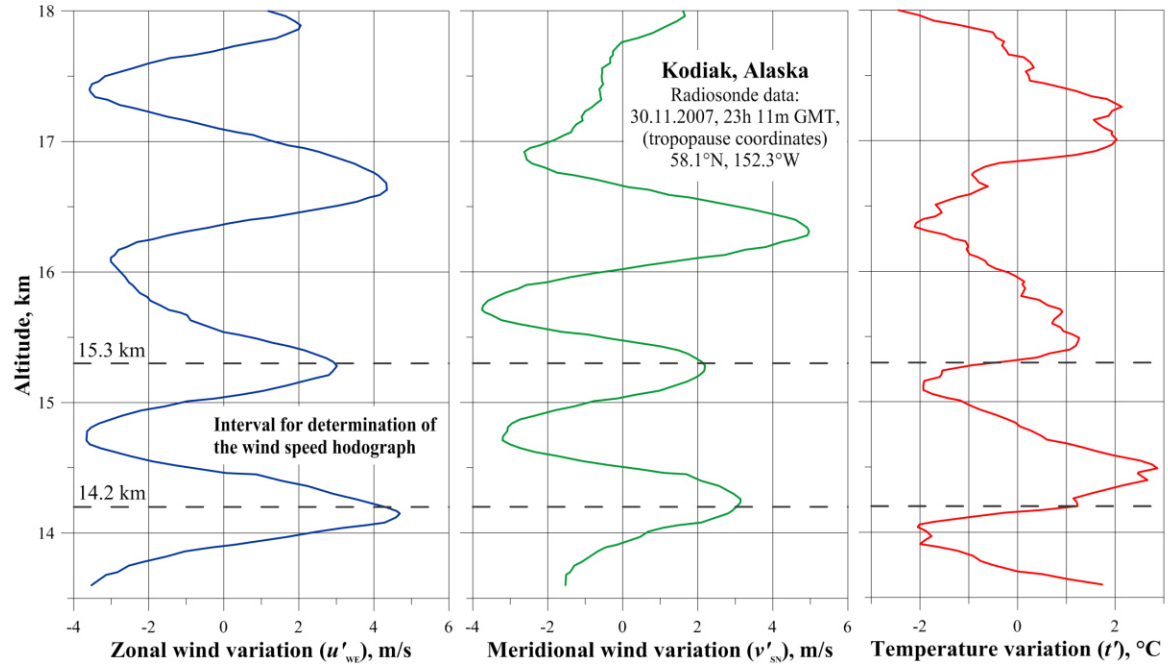

Figure 3. Vertical profiles of the temperature, zonal and meridional wind speed variations obtained from radiosonde measurements on 30 November 2007 in the atmosphere over Kodiak, Alaska. In order to obtain vertical profile of variations, the background profile was subtracted from the corresponding raw profile (see figure 2). Altitude interval (14.2–15.3 km) for determination of the wind speed hodograph is denoted by dashed lines.

Figure 4 demonstrates the elliptical hodograph of horizontal velocity perturbations for an altitude range 14.2–15.3 km. Magnitudes of zonal and meridional wind speed variations are depicted at horizontal and vertical axis, respectively. Dots present raw measurements, ⊙ is the starting hodograph point; numbers near experimental points show altitude at km. Arrow indicates the direction of background velocity $\mathbf{V}_b$ on altitude of ~14.7 km. Polarization ellipse, found from the LSM-approximation of raw data, is shown by the smooth solid line. The values of lengths for the major and minor semi-axes of polarization ellipse are the amplitudes $|u'|$ and $|v'|$ of wind velocity perturbations: $|u'|$=4.86 m/s and $|v'|$=0.46 m/s (HA-method). Note that the last value may be erroneous because it is twice less than accuracy (~1 m/s) of wind speed measurements. For this case in study, the amplitude $|v'|$ and other wave characteristics can be found more accurately using the combined data analysis (CDA-method) of the simultaneous wind speed and temperature measurements and the polarization relation (4) from the work [28]. This improved method of wind speed hodograph analysis is relevant for given case when the intrinsic frequency noticeably exceeds the Coriolis parameter value (see table 1), and it gives a possibility to achieve the minimal errors in results of reconstructing the internal wave characteristics.

Let us illustrate an application of the CDA-method to analyzed data in this case study. The inertial frequency $f=1.24\cdot10^{-4}$ rad/s and amplitude of normalized temperature variations $\left|\hat{T}'\right|=1.13\cdot10^{-2}$ have been calculated. Using polarization relation (4) from the work [28] and experimental values of $|u'|$, $\left|\hat{T}'\right|$, N_b and g, we have found the magnitudes of f/ω and ω: f/ω=0.47 and $\omega=2.64\cdot10^{-4}$ rad/s (intrinsic wave period is $T^{in}=2\pi/\omega$=6.6 hrs). Using the dispersion equation (1) in [28], the values of the intrinsic horizontal phase speed $\left|c-\bar{u}\right|=5.1$ m/s and horizontal wavelength $\lambda_h=\left|c-\bar{u}\right|T^{in}=122$ km are determined. Taking into account relations (2) and (3) from the work [28], we find the amplitudes of horizontal $|v'|$ and vertical $|w'|$ wind speed disturbances: $|v'|$=2.28 m/s and $|w'|=4.4\cdot10^{-2}$ m/s. On the base of well known relationship for IGWs between the intrinsic frequency ω and ground-based frequency σ ($\sigma=\omega+\mathbf{k_hV_b}$), we can obtain the value of σ. Taking into account the direction of the major axis of the polarization ellipse, it is possible to determine the direction of horizontal wave vector $\mathbf{k}_h$ with uncertainty of 180°. The magnitude of angle between the $\mathbf{k}_h$ and $\mathbf{V}_b$ vectors may be equal 16.2° or 163.8° (see figure 4), and it is easy to show that the possible values of wave period in the ground-based system $T_1^{ob}=2\pi/\sigma$ are equal to T_1^{ob} = 6.4 hrs ~ 12 hrs/2 or T_2^{ob} = 2.2 hrs ~ 12 hrs/5. These estimates of the ground-based period T^{ob} support an assumption that the analyzed perturbations of wind speed and temperature (see figure 1) are induced by an internal wave but nor semidiurnal thermal tide.

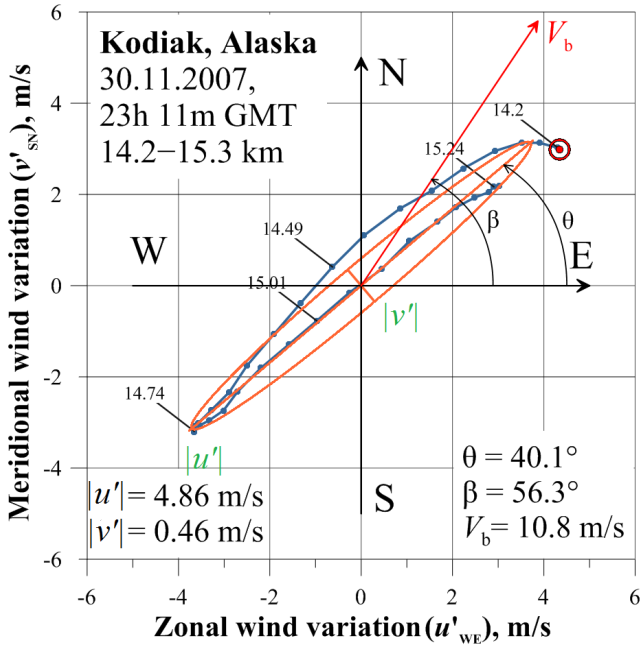

Figure 4. Hodograph of wind speed variations in the altitude interval from 14.2 to 15.3 km (dots – original data, smooth solid curve – fitted polarization ellipse), ⊙ – starting point of hodograph, numbers near experimental points denote corresponding altitudes. The direction of background wind speed $\mathbf{V_b}$ at the altitude of ~14.7 km is indicated by arrow. The vector endpoint of horizontal speed variations rotates anticlockwise with altitude, which indicates the downward energy and upward phase propagation in the Northern Hemisphere. The direction of horizontal wave propagation is parallel to the major axis of the hodograph ellipse with a 180° ambiguity.

Table 1. Internal wave parameters inferred from radiosonde data obtained on 30 November 2007 in the atmosphere over Kodiak, Alaska (58.1°N, 152.3°W, 23h 11m GMT)

Internal wave parameters	**HA-method**	**CDA-method**	**SWA-method**
Vertical wavelength, km	1.1	1.1	1.1
Amplitude of normalized temperature variations, rel. units	$1.13 \cdot 10^{-2}$	$1.13 \cdot 10^{-2}$	$1.13 \cdot 10^{-2}$
Background Brunt-Vaisala frequency, rad/s	$2.58 \cdot 10^{-2}$	$2.58 \cdot 10^{-2}$	$2.58 \cdot 10^{-2}$
Inertial frequency (Coriolis parameter), rad/s	$1.24 \cdot 10^{-4}$	$1.24 \cdot 10^{-4}$	$1.24 \cdot 10^{-4}$
Mean horizontal wind, m/s (in the wave propagation direction)	10.4	10.4	10.4
Amplitude of wind variations parallel to the direction of horizontal wave propagation, m/s	4.86	4.86	4.75
Amplitude of wind variations transverse to the direction of horizontal wave propagation, m/s	0.46	2.28	2.04
Ratio of the inertial to intrinsic frequency, rel. units	$9.5 \cdot 10^{-2}$	0.47	0.43
Intrinsic wave frequency, rad/s	$1.31 \cdot 10^{-3}$	$2.64 \cdot 10^{-4}$	$2.89 \cdot 10^{-4}$
Intrinsic wave period, hours	1.3	6.6	6.0
Intrinsic horizontal phase speed, m/s	4.5	5.1	5.0
Horizontal wavelength, km	22	122	109
Amplitude of vertical wind variations, m/s	$24.5 \cdot 10^{-2}$	$4.4 \cdot 10^{-2}$	$4.8 \cdot 10^{-2}$
Horizontal phase speed, m/s	5.8 or 15.0	5.3 or 15.5	5.4 or 15.4
Ground-based wave period, hours	1.0 or 0.4	6.4 or 2.2	5.6 or 2.0
Relative actual wave amplitude, rel. units	1.07	0.95	0.95
Relative saturated wave amplitude, rel. units	1.00	0.94	0.95
Saturation degree of the wave amplitude	100%	100%	assumed 100%
Horizontal propagation of the wave phase	north-eastward	north-eastward	north-eastward
Vertical propagation of the wave energy	downward	downward	downward
Rotation of the vector endpoint of horizontal speed variations with altitude	anticlockwise	anticlockwise	anticlockwise

In the case of wave energy dissipation, the internal atmospheric waves can change both the value and direction of background wind velocity. Shear and convective instabilities are believed to be the principal processes leading to energy dissipation of IGWs [29, 34]. Convective and shear instabilities cause the internal atmospheric waves to break when their amplitudes outreach the threshold values for the occurrence of corresponding instability. Using equation (7) in the work [28], we derive the relative threshold a=0.94 (CDA-method) for shear instability. Due to the threshold magnitudes, the mechanisms of the IGW saturation are non-linear; therefore, determining the actual wave amplitudes in experiments is important task. Equations (8) from the work [28] give independent identical estimates of the actual IGW amplitude a_e=0.95 (SWA-method) and a_u=0.95 (CDA-method). The

obtained estimates testify that a quality of the temperature and velocity measurements is high, and assumes that polarization equation (4) from the work [28] holds. From the expressions (9) of indicated work, we evaluate the IGW saturation degree $d_e=d_u=1.0=100$ % in two different ways.

Our analysis demonstrates that the improved hodograph technique gives a possibility to identify the internal gravity waves in balloon experiments, and to derive their key parameters and the value of saturation degree in the Earth's atmosphere. For the RO investigations of IGWs in the terrestrial atmospheres [24–27], we apply the saturated wave assumption (SWA-method). In the considered case study we have identified the fully saturated internal wave (d=100%). Comparing the values of internal wave characteristics obtained from radiosonde data by CDA- and SWA-methods shows a remarkably good agreement between them (see table 1). However, the results obtained by the classical hodograph method (HA-method) differ significantly from those indicated above. This discrepancy may be due to large errors of the HA-method in determining the minor semi-axis length of the polarization ellipse. Thus, we see that an upgraded hodograph (CDA-method) method based on combined data analysis of simultaneous wind speed and temperature measurements is useful to achieve the minimal errors in obtained results of reconstructing the internal wave characteristics.

4. Conclusion

An improved hodograph analysis technique to derive the internal gravity wave parameters from radiosonde measurements has been developed. The novelty of our improved method is that it resolves many more waves than can be inferred by the applied classical hodograph technique. This upgraded hodograph method is based on combined analysis of the velocity and temperature measurements. To achieve the minimal errors in results of reconstructing the internal wave characteristics, the polarization relation between the wave wind speed and temperature variations in the Earth's atmosphere has been used. It has been shown that an application of the improved method of wind speed hodograph analysis is especially relevant for cases when the intrinsic frequencies of analyzed IGWs noticeably exceed the Coriolis parameter values.

5. Acknowledgments

This study was made in the framework of state task and it was partially supported by the Russian Foundation for Basic Research (RFBR project no. 19-02-00083 A).

6. References

[1] Thompson R O R Y 1978 *Q. J. R. Meteorol. Soc.* **104** 691.
[2] Woodman R F 1980 *Radio Sci.* **15** 417.
[3] Cot C and Barat J 1986 *J. Geophys. Res*. **91** 2749.
[4] Gardner C S and Voelz D G 1986 *J. Geophys. Res*. **91** 3659.
[5] Vincent R A and Fritts D C 1987 *J. Atmos. Sci.* **44** 748.
[6] Cornish C R and Larsen M F 1989 *J. Atmos Sci*. **46** 2428.
[7] Franke S J and Thorsen D 1993 *J. Geophys. Res*. **98** 18607.
[8] Meriwether J W 1993 *J. Geophys. Res*. **98** 20713.
[9] Sato K 1994 *J. Atmos. Terr. Phys*. **56** 755.
[10] She C Y and Yu J R 1994 *Geophys. Res. Lett.* **21** 1771.
[11] Cho J Y N 1995 *J. Geophys. Res*. **100** 18727.
[12] Swenson G R, Gardner C S and Taylor M J 1995 *Geophys. Res. Lett.* **22** 2857.
[13] Eckermann S D 1996 *J. Geophys. Res.* **101** 19169.
[14] Gavrilov N M, Fukao S, Nakamura T, Tsuda T, Yamanaka M D and Yamamoto M 1996 *J. Geophys. Res*. **101** 29511.
[15] Namboothiri S P, Tsuda T, Tsutsumi M, Nakamura T, Nagasawa C and Abo M 1996 *J. Geophys. Res*. **101** 4057.
[16] Walterscheid R L, Hecht J H, Vincent R A, Reid I M, Woithe J and Hickey M P 1999 *J. Atmos. Sol.-Terr. Phys.* **61** 461.
[17] Preusse P, Eckermann S D and Offermann D 2000 *Geophys. Res. Lett.* **27** 3877.

[18] Hecht J H, Walterscheid R L, Hickey M P and Franke S J 2001 *J. Geophys. Res*. **106** 5181.
[19] Hu X, Liu A Z, Gardner C S and Swenson G R 2002 *Geophys. Res. Lett.* **29** 2169, doi:10.1029/2002GL014975.
[20] Ern M, Preusse P, Alexander M J and Warner C D 2004 *J. Geophys. Res.* **109** D20103.
[21] Serafimovich A, Hoffmann P, Peters D and Lehmann V 2005 *Atmos. Chem. Phys.* **5** 295.
[22] Rauthe M, Gerding M, Hoffner J and Lubken F-J 2006 *J. Geophys. Res.* **111** D24108.
[23] Rauthe M, Gerding M and Lubken F-J 2008 *Atmos. Chem. Phys*. **8** 6775.
[24] Gubenko V N, Pavelyev A G and Andreev V E 2008 *J. Geophys. Res.* **113** D08109, doi: 10.1029/2007JD008920
[25] Gubenko V N, Pavelyev A G, Salimzyanov R R and Pavelyev A A 2011 *Atmos. Meas. Tech.* **4** 2153, doi: 10.5194/amt-4-2153-2011.
[26] Gubenko V N, Pavelyev A G, Salimzyanov R R and Andreev V E 2012 *Cosmic Res*. **50** 21, doi: 10.1134/S0010952512010029.
[27] Gubenko V N, Kirillovich I A and Pavelyev A G 2015 *Cosmic Res.* **53** 133, doi: 10.1134/S0010952515020021.
[28] Gubenko V N and Kirillovich I A 2018 *Sol.-Terr. Phys.* **4** 41, doi: 10.12737/stp-42201807.
[29] Fritts D C and Alexander M J 2003 *Rev. Geophys.* **41** 1, doi:10.1029/2001RG000106.
[30] Zink F and Vincent R A 2001 *J. Geophys. Res.* 2001 **106** 10275.
[31] Gill A E 1982 *Atmosphere-Ocean Dynamics* (New York, London, Paris: Academic Press).
[32] Pfister L, Chan K R, Bui T P, Bowen S, Legg M, Gary B, Kelly K, Proffitt M and Starr W 1993 *J. Geophys. Res.* **98** 8611.
[33] Hines C O 1989 *J. Atmos. Sci.* **46** 476.
[34] Fritts D C 1989 *Pure Appl. Geophys.* **130** 343.